

Microstructure and Property of Al-FeCoNiCrAl High Entropy Alloy Composite Coating on Ti-6Al-4V During Annealing Using MA Method

SU Ningning, FENG Xiaomei*, ZANG Jiajun, SUN Jing, LI Huan

College of Materials Science and Technology, Nanjing University of Aeronautics and Astronautics, Nanjing 211106, P. R. China

(Received 9 March 2020; revised 26 April 2020; accepted 18 May 2020)

Abstract: Al-FeCoNiCrAl high entropy alloy (HEA) composite coatings were prepared on Ti-6Al-4V via high-energy mechanical alloying (MA). The microstructures and phase composition of the coatings were studied. A continuous and dense coating could be fabricated at a ratio of 35% (weight fraction) Al-FeCoNiCrAl after 4 h milling. The results showed that the thickness of the composite coatings increased first and then decreased with the increase of milling time. And the hardness of coating increased with the increase of milling time. The phase changed during the annealing process. Part of the initial body-centered cubic (BCC) phase of the composite coatings changed into the $L1_2$ phase, $(\text{Ni}, \text{Co})_3\text{Al}_4$ and σ phase after annealing above 550 °C. Ordered BCC was found in the coatings after annealing above 750 °C. Only BCC and ordered BCC appeared in coatings after annealing above 1 050 °C. The hardness of the coatings after annealing at 550 °C and 750 °C was higher than before because of spinodal decomposition and high hardness σ phase. The hardness of the coatings after annealing at 1 050 °C decreased because residual stress released.

Key words: high entropy alloys; Ti-6Al-4V alloy; mechanical alloying; composite coating; annealing process;

CLC number: TF125 **Document code:** A **Article ID:** 1005-1120(2020)03-0481-09

0 Introduction

High entropy alloys (HEAs) are preferentially defined as alloys that composed of more than five principal elements, each with an atomic percentage between 5% and 35%^[1]. Several important core effects, such as high entropy, severe lattice distortion, sluggish diffusion and cocktail effect, were exhibited in HEAs^[2]. With compositional complexity and rich microstructural variation, HEAs exhibit high hardness and other properties^[3-5].

Titanium and its alloys have been extensively applied in aeronautical manufacture, automotive and other fields due to their high specific strength and excellent corrosion resistance^[6-7]. Various surface modification methods, such as the magnetron sputtering, laser cladding, plasma spraying, etc, have

been widely applied to Ti-6Al-4V for improving their performance^[8-12]. However, these methods have disadvantages, such as high cost, complex operation of equipment for experiment, unstable quality of coating and low preparation efficiency, etc.

Mechanical alloying (MA) method is a solid-state and non-equilibrium processing technique^[13]. The preparation of continuous coatings via MA relies on cold welding of solid-state powder particles. The advantages of the MA method include the lower cost, high ambient temperature, simple equipment, high efficiency-preparation and favorable adhesion of coatings, etc. Considerable research efforts have been devoted to fabricating the composite coatings on bulk materials by MA^[14-20], such as Al-Ni, Al-Cr, Al-Si, Al-Ti, etc.

Therefore, it is imperative to investigate the preparation of HEA composite coatings on titanium

*Corresponding author, E-mail address: fengxm_nuaa@hotmail.com.

How to cite this article: SU Ningning, FENG Xiaomei, ZANG Jiajun, et al. Microstructure and property of Al-FeCoNiCrAl high entropy alloy composite coating on Ti-6Al-4V during annealing using MA method[J]. Transactions of Nanjing University of Aeronautics and Astronautics, 2020, 37(3):481-489.

<http://dx.doi.org/10.16356/j.1005-1120.2020.03.014>

alloys via MA method. In this paper, 35% (weight fraction) Al-FeCoNiCrAl composite coatings have been fabricated on Ti-6Al-4V by MA. The Al-FeCoNiCrAl composite coatings belong to the ductile-brittle system, in which the ductile Al is a bonding agent and the FeCoNiCrAl particle could improve the performance of coatings. This work provides practical preparation of HEA composite coatings by MA method. The microstructures, phases and compositions of the synthesized coatings were characterized. The phase transformation and micro-hardness of composite coatings during the annealing process were characterized as well.

1 Experimental Procedure

The Al-FeCoNiCrAl coatings were prepared using a Fritsch Pulverisette6 planetary mono mill. The Ti-6Al-4V alloy was cut by laser into blocks with a dimension of 12 mm×12 mm×3 mm. The surface was polished by silicon carbide abrasive paper and then washed by ultrasonic cleaning with absolute ethyl alcohol.

The original powder used in this paper were argon atomized FeCoNiCrAl (99%, 500 mesh) powder and pure aluminum (99.9%, 200 mesh) powder, and the chemical composition of FeCoNiCrAl powder is shown in Table 1. The coating preparing processes were conducted in a stainless steel grinding vial of 700 ml. 10.5 g Al powder, 19.5 g FeCoNiCrAl HEA powder, 4 blocks of substrates and 300 g grinding balls were put into the grinding vial before MA, and the schematic illustration is shown in Fig.1. The diameter of grinding balls is 6 mm and 8 mm for improving the efficiency of ball-powder-substrate effects. The coatings prepared at 2 h, 4 h, 6 h and 8 h were used to compare the phase compositions and properties during milling duration. Other parameters including speed of 350 r/min and the ball-to-powder ratio of 10:1 remained constant. The milling processes were performed in the ambient atmosphere and no process control agent was added to the vial. In order to prevent an excessive temperature rise occurred in the vial, the operation of 20 min ball milling was followed by 10 min of cooling. Then

the specimens were annealed at 550 °C, 750 °C, 850 °C and 1 050 °C for 2 h under an argon atmosphere, to avoid samples oxidation.

Table 1 Chemical composition of FeCoNiCrAl powder %

Element	Fe	Ni	Co	Cr	Al	O	N
Weight percentage	Bal.	23.62	23.76	20.71	8.81	0.030 7	0.003 2

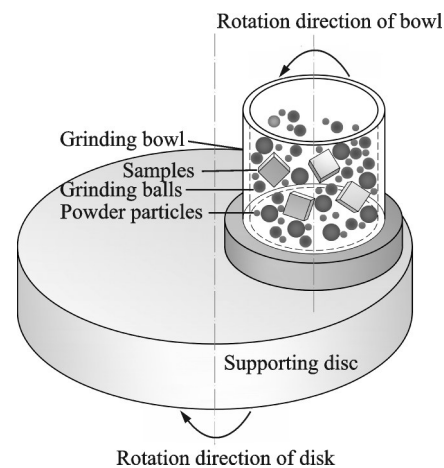


Fig.1 Schematic of experimental apparatus

The cross-section of specimens were obtained by spark-erosion wire cutting method and then handled by sanding and polishing according to the standard procedure. Microstructures and chemical compositions of the coatings were observed by a scanning electron microscopy (FESEM, HITACHI S-4800 Field emission) equipped with an energy dispersive X-ray spectrometer (EDX, Bruker XFlash 5030).

The phase structures of the coatings were identified by X-ray diffraction (XRD, Bruker D8) with Cu K α radiation ($\lambda = 0.154\ 059\ 8\ \text{nm}$) at 40 kV and 40 mA, using a continuous scan mode over the wide angle 2θ range of 20°—90°.

The NETZSCH STA 449F3 instrument was used to get the TG-DSC curve at a constant heating rate of 10 K/min ranging from 30 °C (303 K) to 1 200 °C (1 473 K) under Ar atmosphere to check the phase changing temperature and thermal stability. Al₂O₃ crucible was used in this experiment.

A HXS-1000A micro-hardness tester was utilized to determine the Vickers hardness of the coatings and substrates, with a load of 0.1 kg and an in-

dentation time of 15 s. The micro-hardness was tested along the profiles of the coated samples from the near-surface to the inner substrates.

2 Results and Discussion

2.1 Microstructures and composition

Fig.2 shows the cross-sectional microstructures of 35% (weight fraction) Al-FeCoNiCrAl coatings on Ti-6Al-4V substrate under different milling times. It can be seen that all coatings exhibit mottled structures and the gray areas represent the HEA particles while the dark areas are the Al particles. Besides, FeCoNiCrAl particles are angular with non-uniformly dimensions. With the increase of milling time, the thickness of the coatings first increases and then decreases. The thickness of the coating after 4 h of ball milling reaches the maximum value. When the milling time prolongs to 8 h, the cracks and micro-holes are formed in the coatings as shown in Fig.2(d).

The outer light layer is hard-worked Al which will be analyzed later by energy dispersive spectrum (EDS). The deposition of particles relies on the ball-particle-substrate effects, which could result in cold

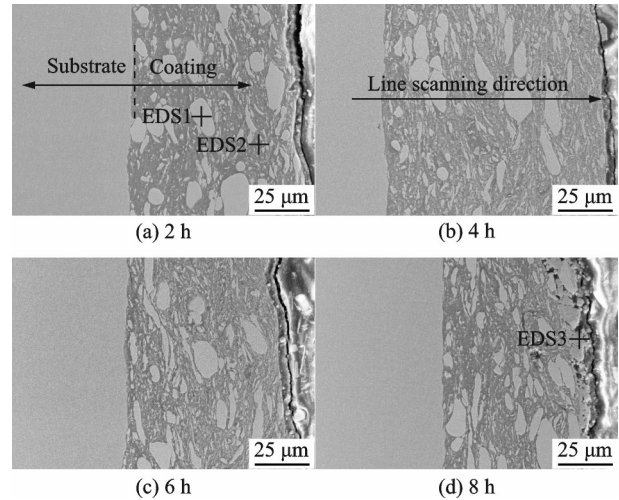


Fig.2 Cross-section microstructures of 35% (weight fraction) Al-FeCoNiCrAl coatings under different milling time

welding of particles and manufacture continuous coatings^[13]. With the increase of milling time, the particles and the coating work hardened^[21]. The flaking of coating and the deposition of work-hardened particles on the harder coatings would result in micro-holes and cracks, and the thickness of the coatings will reduce due to repeated collision of milling balls.

Figs.3(a)–(c) are the EDS results of position

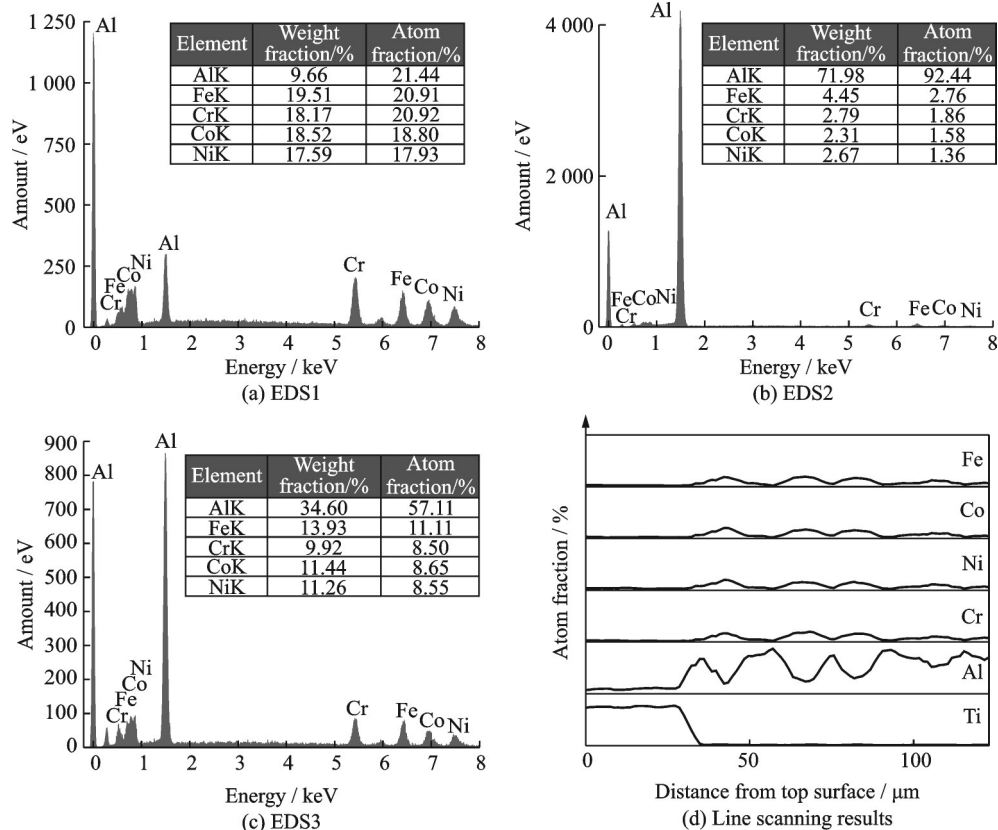


Fig.3 Corresponding EDS results of the coatings in Fig.2

1—3 as shown in Figs.2(a) and (d). The results show that the gray particles are FeCoNiCrAl HEA and the dark particles are Al particles. Fig.3(c) shows that the layer is composed of homogeneous Al-FeCoNiCrAl composite particles, which indicate the Al dissolved in the HEA. Fig.3(d) shows the EDS line scanning results obtained from the surface to the inner substrate of the coatings after 8 h milling and the EDS line scanning result is carried out from the surface to the inner substrate. Severe fluctuations of the main element contents indicate the composite structure in the coatings. The fluctuations of Fe, Co, Ni, and Cr in the coatings are similar. The closer to the coating surface, the more uniform the element distribution. The change of the proportion of Al is opposite to the change of Fe, Co, Ni and Cr.

Fig.4 shows the XRD patterns of the raw powder and the top surface of the composite coatings. The phase composition of the coatings is Al and FeCoNiCrAl HEA. Body-centered cubic (BCC) and face-centered cubic (FCC) structures of FeCoNiCrAl powder transformed into BCC structure after 2 h milling duration, which is due to that Al diffused to the HEA during MA^[22]. The peak of Ti disappearing in MA-4 h and MA-6 h indicates that the substrate has been covered completely, and continuous and dense coatings have formed on it. The diffraction peak of Al and HEA gradually decreases during the milling duration. However, the diffraction peak of Al after 8 h milling disappears because the composite Al-FeCoNiCrAl particles have ad-

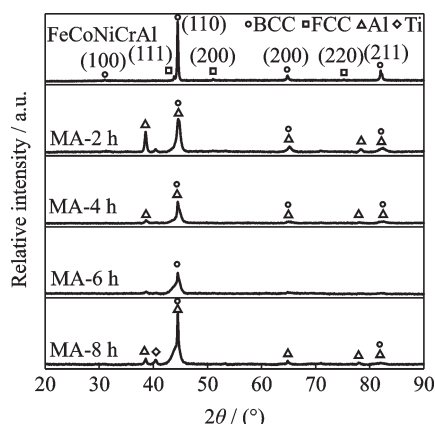


Fig.4 XRD patterns of HEA and coatings using different milling time

hered to the top surface of the coatings.

2.2 Annealing process

The simultaneous thermal analysis method was used for 35% (weight fraction) of Al-FeCoNiCrAl powders after milling for 4 h. Fig.5 shows the differential scanning calorimetry (DSC), thermogravimetry analysis (TG) and differential thermogravimetry analysis (DTG) curves of the powders. In the DSC curve, the endothermic long line from 50 °C to 365 °C could be associated with thermal transients. Long endothermic curves can be associated with the gradual collapse of the crystalline structure. The phase change is characterized by the endothermic peaks of 387.8 °C, 629.0 °C and 926.6 °C.

The TG curve in Fig.5 indicates the weight change of 4 h mechanically alloyed 35% of Al-FeCoNiCrAl powder. The weight decreases first and then increases twice. 0.37% of weight gain after the first weight changing. 4.64% of total weight gain is achieved when the temperature reaches 1 200 °C. Weight gain could be attributed to surface oxidation. The first peak of the DTG curve is 633.9 °C of 0.11%/min. Another peak is 926.9 °C of 0.24%/min. These peaks are related to the phase transformation, which corresponds to the endothermic peaks of 629.0 °C and 926.6 °C in the DSC.

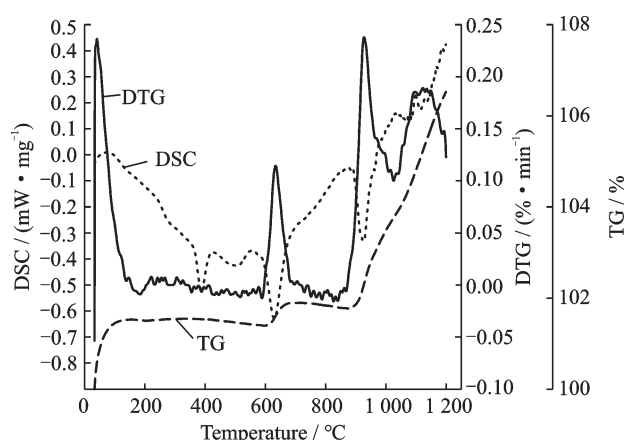


Fig.5 DSC, TG and DTG curves of Al-FeCoNiCrAl compound powder ball milled for 4 h

Fig.6 shows the XRD patterns of 35% (weight fraction) Al-FeCoNiCrAl coating surfaces after annealing at different temperatures. A super-saturated solid solution is easily formed during MA, and the

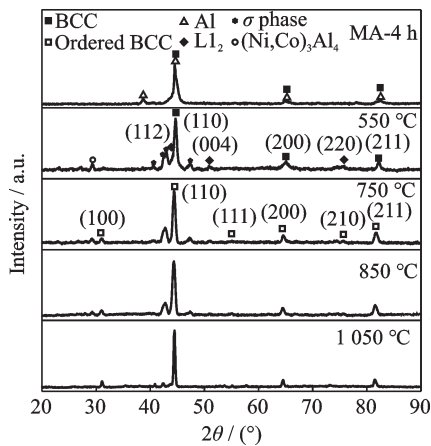


Fig.6 XRD patterns of the top surface of the coating annealing at different temperatures

annealing process makes phase precipitated in the coating. The mixing enthalpy between Ni and Al is relatively negative, so Ni and Al are easy to combine^[23]. New diffraction peaks of Ni₃Al prototype L₁₂ phase and Fe-Cr-Co type σ phase are formed after annealing at 550 °C along with the initial BCC phase^[24]. The unstable precipitated L₁₂ phase is easy to transform to ordered BCC with the increase of annealing temperature. So the (Ni, Co)₃Al₄, BCC phase, ordered BCC and σ phase are found in the coating after annealing at 750 °C. Diffraction peaks of the coating after annealing at 850 °C are similar to 750 °C. The phase of the coating after annealing at 1 050 °C is BCC and ordered BCC. Other unstable phases like (Ni, Co)₃Al₄ and σ phase are decomposed after annealing at 1 050 °C of 2 h.

Fig.7 is cross-section microstructures of Al-Fe-CoNiCrAl coatings after annealing at different temperatures. The coating after annealing at 550 °C is composed of black Al particles and bright FeCoNiCrAl particles, which are similar to those coating before annealing. Bright Al particles in the coating after annealing at 750 °C are not obvious as the coating before annealing. Narrow FeCoNiCrAl particles grow larger than those before annealing, because the Al particles are melted and dissolved into HEA particles during annealing. The particle in the coating after annealing at 850 °C is the same as the coating after annealing at 750 °C. The interface between the particles in the coating disappears after annealing at 1 050 °C.

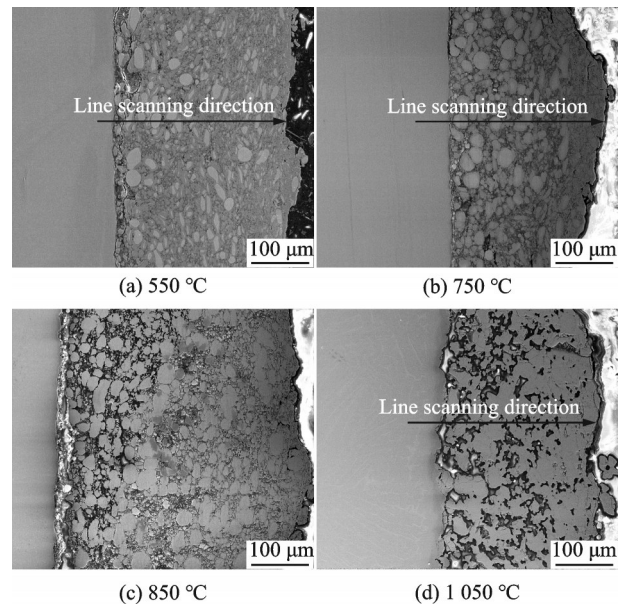


Fig.7 Cross-section of the sample after annealing for 2 h at different temperatures

The cracks between the coating and TC4 substrate are generated after annealing at 550 °C as shown in Fig.7(a). That is attributed to the fact that the precipitated phase reduces the bonding between the coating and substrate. The cracks are found in the coatings after annealing at 750 °C and 850 °C as shown in Figs.7(b) — (c). Fig.7(d) shows that there is no crack between the composite coating and the TC4 substrate in the coating after annealing at 1 050 °C, because the precipitated phase is decomposed after annealing at such high temperature.

Fig.8 shows the EDS line scanning results of the Al-FeCoNiCrAl coatings annealing at different temperatures. The EDS line scanning is carried out from the TC4 substrate to the coating surface. With the increase of annealing temperature, the distribution of the Al element in the coating becomes more and more uniform, especially these areas close to the top surface. This reason is mainly that the annealing temperature is higher than the melting point of Al, which makes it easier for liquid Al to diffuse^[25].

The distributions of Fe, Co, Ni and Cr elements of the coating after annealing at different temperatures shown by the EDS linear scan result are basically the same. However, the changing law of Cr in the coating annealing at 1 050 °C is not similar to Fe, Ni and Co, but consistent with Al, because

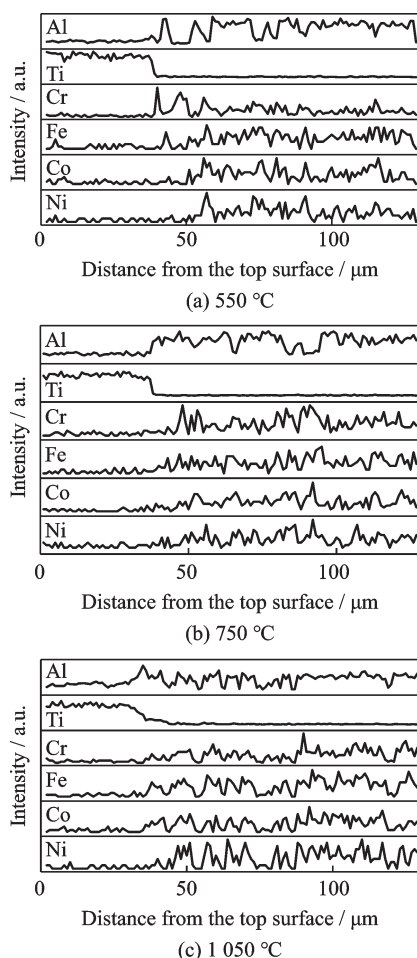


Fig.8 Corresponding linear scanning results of cross-section morphology of the coating annealing at different temperatures

the enthalpy of Al and Ni is relatively negative, and Al, Ni-rich ordered BCC formed. The element content of Ti in the interface of the coating is flatter with the annealing temperature increased, which proves that Ti diffuses from the TC4 substrate to the coating, and becomes more intense as the annealing temperature increases.

2.3 Properties

Fig.9 shows the cross-section hardness of the Al-FeCoNiCrAl coating under different milling time. The maximum micro-hardness value is obtained near the surfaces of coatings. The micro-hardness values of the coating increase with the increase of milling duration. The maximum micro-hardness value of the coating after milling 8 h is 605.6 HV_{0.1}, much higher than the maximum micro-hardness value of the coating after 2 h milling, which is 402.7 HV_{0.1}. The hardness of the substrate increases with the in-

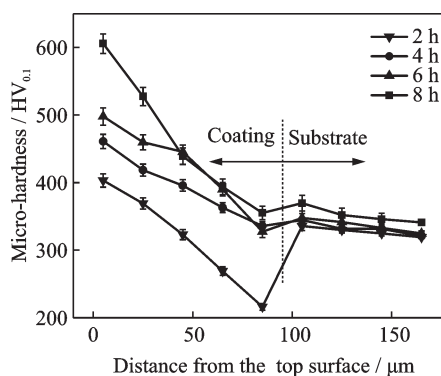


Fig.9 Variations of micro-hardness of the coating under different milling duration along cross-section from the top surface to the inner substrate

crease of milling time, which is due to that the substrate, composite coating and powder gradually work harden under the collision of milling balls during MA and the grain of the coating and substrate is refined as well. The coating is denser under the collision of the milling ball, and then the hardness of the coating and substrate increases. The hardness of the inner layer of the coating after milling for 2 h is lower than the substrate because the Al cold-welded on the coating surface is soft due to lack of work hardening.

Fig.10 shows the hardness of these Al-FeCoNiCrAl coatings after annealing at different temperatures. Annealing makes the work hardening effect of the coating weaken. The grains in the coating recover to recrystallize, which reduces the hardness of the coating. However, the hardness of the coating surface after annealing at 550 °C is higher than before, because the hard σ phase could increase the

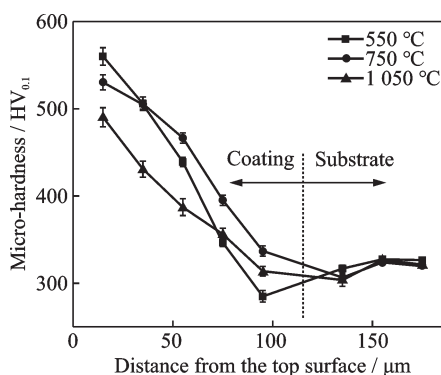


Fig.10 Variations of micro-hardness of the coatings along cross-section from the top surface to the inner substrate after different annealing temperatures

hardness of coatings^[26]. The maximum hardness of the coatings annealing at 750 °C is 559.9 HV_{0.1}, which is much higher than before. Ordered BCC is discovered after the annealing process, spinodal decomposition could increase the hardness of the coatings as well^[27]. The hardness of the coatings after annealing at 1 050 °C is less than that before, because the σ phase dissolves, and the grain grows after annealing at such high temperature. Residual stress is released with the increase of the annealing temperature. As a result, the hardness of the coating annealed at 1 050 °C is less than that before. However, the hardness of the inner layer in the coatings annealed at 1 050 °C is higher than before, because Ti diffuses from the TC4 into the coating.

3 Conclusions

Al-FeCoNiCrAl composite coatings were successfully synthesized on the Ti-6Al-4V alloy substrate by MA. The effect of milling duration and element ratio for the Al-FeCoNiCrAl coating was studied. The microstructure and phase of coatings after annealing were discussed. Based on the above results, the following conclusions can be drawn:

(1) The TC4 substrate was fully covered with the Al-FeCoNiCrAl coating after MA treatment. The coatings were composite structure made up of FeCoNiCrAl particles and the ductile Al. The closer to the coating surface, the more uniform the structure of the coatings, and the less the Al content.

(2) Milling time had a significant effect on the preparation of the Al-FeCoNiCrAl coating. The thickness of the composite coatings increased first and then decreased with the increase of milling time. The sample after milling for 4 h showed a better morphology and the thickest composite structure. Defects were generated in the coating after milling for 8 h.

(3) The TG-DSC curve of Al-FeCoNiCrAl powder indicated that the phase change occurred at 387.8 °C, 629.0 °C and 926.6 °C. The (Ni, Co)₃Al₄, L1₂ phase and σ phase were found after annealing above 387.8 °C. L1₂ phase transformed into ordered

BCC in the coating above 629.0 °C. Only BCC and ordered BCC were found in the coating above 926.6 °C.

(4) As the annealing temperature increased, the more uniformly the elements were distributed in the coating. Because Al diffused to the FeCoNiCrAl in a liquid state when the annealing temperature was higher than the melting point of Al. As the annealing temperature increased, Ti diffused severer. The change law of Fe, Co, Ni and Cr was close after annealing at 550 °C and 750 °C.

(5) The maximum micro-hardness value of the Al-FeCoNiCrAl coatings was obtained near the top surfaces. The hardness of the coatings increased with the increase of milling duration. The coating after annealing at 750 °C had a higher hardness than before, which was due to the hardness σ phase and spinodal decomposition. The coating after annealing at 1 050 °C was harder than before, because the residual stress and the effect of work hardening were released.

Reference

- [1] YE H J W, CHEN S K, LIN S J, et al. Nanostructured high-entropy alloys with multiple principal elements: Novel alloy design concepts and outcomes[J]. *Advanced Engineering Materials*, 2004, 6(5): 299-303.
- [2] YE H J W. Recent progress in high-entropy alloys[J]. *Annales de Chimie Science des Matériaux (Paris)*, 2006, 31(6): 633-648.
- [3] HASAN M N, LIU Y F, AN X H, et al. Simultaneously enhancing strength and ductility of a high-entropy alloy via gradient hierarchical microstructures[J]. *International Journal of Plasticity*, 2019, 123: 178-195.
- [4] NOEBE R D, BOWMAN R R, NATHAL M V. Physical and mechanical properties of the B2 compound NiAl[J]. *International Materials Reviews*, 1993, 38(4): 193-232.
- [5] SONKUSARE R, JAIN R, BISWAS K, et al. High strain rate compression behaviour of single phase Co-CuFeMnNi high entropy alloy[J]. *Journal of Alloys and Compounds*, 2020, 823: 153763.
- [6] LUTJERING G, WILLIAMS J C. *Titanium*[M]. [S.l.]: Springer Science & Business Media, 2007.

- [7] TAO Jie, HUANG Zhendong, LIU Hongbing, et al. Preparation and characterization of anti-oxidation enamel coating for Ti-based alloys at high temperature[J]. *Journal of Nanjing University of Aeronautics & Astronautics*, 2010, 42(4): 505-509. (in Chinese)
- [8] HAMDI D A, JIANG Z T, NO K, et al. Biocompatibility study of multi-layered hydroxyapatite coatings synthesized on Ti-6Al-4V alloys by RF magnetron sputtering for prosthetic-orthopaedic implant applications[J]. *Applied Surface Science*, 2019, 463: 292-299.
- [9] LI C G, ZENG M, LIU C M, et al. Microstructure and tribological behavior of laser cladding TiAlSi composite coatings reinforced by alumina-titania ceramics on Ti-6Al-4V alloys[J]. *Materials Chemistry and Physics*, 2020. DOI: <https://doi.org/10.1016/j.matchemphys.2019.122271>.
- [10] YANG Q, ZHOU W L, ZHENG X B, et al. Investigation of shot peening combined with plasma-sprayed CuNiIn coating on the fretting fatigue behavior of Ti-6Al-4V dovetail joint specimens[J]. *Surface and Coatings Technology*, 2019, 358: 833-842.
- [11] CHEN Y, DING L Y, FU Y C, et al. Dry grinding of titanium alloy using brazed monolayer CBN wheels coated with graphite lubricant[J]. *Transactions of Nanjing University of Aeronautics & Astronautics*, 2014, 31(1): 1-15.
- [12] BAI Jingying, WEN Chen, CHEN Xiaohong, et al. Effect of plasma nitriding treatment on performance of TC4 titanium alloys[J]. *Journal of Nanjing University of Aeronautics & Astronautics*, 2018, 50(S2): 48-51. (in Chinese)
- [13] SURYANARAYANA C. Mechanical alloying and milling[J]. *Progress in Materials Science*, 2001, 46(1/2): 1-184.
- [14] ZADOROZHNYI V Y, SHAHZAD A, PAVLOV M D, et al. Synthesis of the Ni-Al coatings on different metallic substrates by mechanical alloying and subsequent laser treatment[J]. *Journal of Alloys and Compounds*, 2017, 707: 351-357.
- [15] CHEN C, ZHANG J P, DUAN C Y, et al. Investigation of Cr-Al composite coatings fabricated on pure Ti substrate via mechanical alloying method: Effects of Cr-Al ratio and milling time on coating, and oxidation behavior of coating[J]. *Journal of Alloys and Compounds*, 2016, 660: 208-219.
- [16] CHEN C, FENG X M, SHEN Y F. Oxidation behavior of a high Si content Al-Si composite coating fabricated on Ti-6Al-4V substrate by mechanical alloying method[J]. *Journal of Alloys and Compounds*, 2017, 701: 27-36.
- [17] SHAHZAD A, ZADOROZHNYI V Y, PAVLOV M D, et al. Deposition of the Ti-Al coatings on different metallic substrates by mechanical alloying and subsequent laser treatment[J]. *Journal of Alloys and Compounds*, 2018, 731: 1295-1302.
- [18] TIAN Y, SHEN Y F, LU C Y, et al. Microstructures and oxidation behavior of Al-CrMnFeCoMoW composite coatings on Ti-6Al-4V alloy substrate via high-energy mechanical alloying method[J]. *Journal of Alloys and Compounds*, 2019, 779: 456-465.
- [19] EBRAHIM M R, SHEHATA O S, FATAH A H A. Electrochemical behavior of Al₂O₃/Al composite coated Al electrodes through surface mechanical alloying in alkaline media[J]. *Current Applied Physics*, 2019, 19(4): 388-393.
- [20] YANG T F, XIA S Q, LIU S, et al. Effects of Al addition on microstructure and mechanical properties of Al₁CoCrFeNi high-entropy alloy[J]. *Materials Science and Engineering: A*, 2015, 648: 15-22.
- [21] ZUO M, ZHAO D G, WANG Z Q, et al. Investigation on WC-Al composite coatings of AZ91 alloy by mechanical alloying[J]. *Materials Science and Technology*, 2015, 31(9): 1051-1057.
- [22] WANG W R, WANG W L, WANG S C, et al. Effects of Al addition on the microstructure and mechanical property of Al₁CoCrFeNi high-entropy alloys[J]. *Intermetallics*, 2012, 26: 44-51.
- [23] TAKEUCHI A, INOUE A. Classification of bulk metallic glasses by atomic size difference, heat of mixing and period of constituent elements and its application to characterization of the main alloying element[J]. *Materials Transactions*, 2005, 46(12): 2817-2829.
- [24] SHIVAM V, BASU J, PANDEY V K, et al. Alloying behaviour, thermal stability and phase evolution in quinary AlCoCrFeNi high entropy alloy[J]. *Advanced Powder Technology*, 2018, 29(9): 2221-2230.
- [25] MURRAY J L, MCALISTER A J. The Al-Si (aluminum-silicon) system[J]. *Bulletin of Alloy Phase Diagrams*, 1984, 5(1): 74-84.
- [26] MOHANTY S, MAITY T N, MUKHOPADHYAY S, et al. Powder metallurgical processing of equiatomic AlCoCrFeNi high entropy alloy: Microstructure and mechanical properties[J]. *Materials Science*

& Engineering A, 2016, 679: 299-313.

- [27] TONG C J, CHEN M R, YEH J W, et al. Mechanical performance of the Al₂CoCrCuFeNi high-entropy alloy system with multiprincipal elements[J]. Metallurgical & Materials Transactions A, 2005, 36 (5) : 1263-1271.

Authors Mr. SU Ningning received the B.S. degree in Shandong University of Technology in June 2017. He joined in the College of Materials Science and Technology of Nanjing University of Aeronautics and Astronautics in September 2017, where he is pursuing the M.S. degree. His major is materials processing engineering and his research focuses on the preparation of high entropy alloy composite coating.

Dr. FENG Xiaomei received the B.S. and M.S. degrees in Taiyuan University of Technology, Taiyuan, China, in 1992 and 2000, respectively. She received the Ph.D. degree

in Institute of Physics, Chinese Academy of Sciences, in 2008. From 2008 to 2010, she was a postdoctoral researcher at the Delft University of Technology, Holland. From 2010 to present, she has been with the College Materials Science and Technology, Nanjing University of Aeronautics and Astronautics. Her research has focused on magnetic functional materials, the relationship between material structures and performances.

Author contributions Dr. FENG Xiaomei designed the study. Mr. SU Ningning performed the experiments and wrote the paper. Mr. ZANG Jiajun reviewed the manuscript. Ms. SUN Jing contributed to background of the study. Mr. LI Huan manufactured the samples. All authors commented on the manuscript draft and approved the submission.

Competing interests The authors declare no competing interests.

(Production Editor: XU Chengting)

退火对 Ti-6Al-4V 表面 MA 法制备 Al-FeCoNiCrAl 高熵合金复合涂层的组织及性能研究

苏宁宁, 冯晓梅, 臧家俊, 孙静, 李焕

(南京航空航天大学材料科学与技术学院, 南京 211106, 中国)

摘要:采用机械合金化法在 TC4 钛合金基体上成功制备了均匀致密的 Al-FeCoNiCrAl 高熵合金复合涂层, 研究了退火对复合涂层物相组成和性能的影响, 建立起退火温度与复合涂层物相演变和性能之间的内在关系。结果表明: 涂层厚度随着球磨时间增加先增加后减小, 并且涂层硬度随着球磨时间增加而增加。涂层的物相随退火温度变化而变化, 复合涂层为 BCC 相, 550 °C 退火 2 h 后涂层中生成了 L1₂ 相, σ 相和 (Ni, Co)₃Al₄。750 °C 退火后涂层中生成有序 BCC 相。1 050 °C 退火后涂层中仅存 BCC 相和有序 BCC 相。在 550 °C 和 750 °C 退火后涂层的硬度略微升高, 1 050 °C 退火后涂层硬度降低。

关键词:高熵合金; 钛合金; 机械合金化; 复合涂层; 退火处理